



## ARTICLE

# Simulation of Temperature Effects on Concrete Residual Strength of the Slab-Column Connections

Wenchen Ma\*

Department of Civil and Environmental Engineering and Construction, University of Nevada, Las Vegas, 4505 S. Maryland Parkway, Las Vegas, NV 89154, USA

## ARTICLE INFO

*Article history*

Received: 12 October 2019

Revised: 13 October 2019

Accepted: 19 October 2019

Published Online: 31 October 2019

*Keywords:*

Temperature effects

Residual strength of concrete

Non-linear behavior of concrete

## ABSTRACT

Finite element simulations were conducted to explore the effects of high temperatures on the loading capacity of slab-column connection for the concrete flat-plate structures by the finite element analysis software ABAQUS. The structure used for the simulation is a slab which thickness is 150 mm with a 300 mm square column in the middle of slab, the column height is 450mm. The size of this slab is the same as experiments conducted by previous paper[1]. Based on the results of simulation, the punching capacity of this structure not experienced high temperature can be predicted with very good accuracy. But the result from simulations underestimated the loading capacity of the structure after it has been cooled by around 10%. This phenomenon is a little bit conflicts with the known experimental results, however, it can be adjusted by modify the material parameters built-in the software. This article is focus on how to best simulate the concrete behavior for both linear and nonlinear part under the room temperature and cooling after experience a very high temperature.

## 1. Introduction

Reinforced concrete flat slab is a commonly used for both office buildings, residential and parking garages, which consists a uniform thickness slab supported directly on the columns. By this way, the construction cost and architectural versatility will be very low. Unexpected fire will threaten the reliability of flat plate structure due to combined of bending and shear; it will increase the probability of failure of slab-column joint and may cause the progressive collapse of whole structure in the end. One flat slab parking garage collapsed leads 7 people dead in this catastrophe in Switzerland. The reason of collapse is due to fire lasted for more than 90 minutes,

this makes the punching capacity decrease at the slab-column joint<sup>[2,3]</sup>. If both the linear and nonlinear behavior of concrete before and after experienced high temperature can be simulated by the software accurately, it can prevent disaster like this and give suggestion about the probability of structural failure.

## 2. Heat Transfer Analysis

The author using ABAQUS to simulate the behavior of this structure during the heating and loading process because this software can simulate very well in many areas such as: dynamics, static loading, temperature and so on<sup>[4,5]</sup>. The square slab shown in Figure 1 is the structure simulated by ABAQUS, the model using element type

\*Corresponding Author:

Wenchen Ma,

Male, born July 1992, is a Ph.D student majoring in civil engineering concentrate on structural engineering at UNLV;

E-mail: [maw2@unlv.nevada.edu](mailto:maw2@unlv.nevada.edu).

C3D8T. Eight layers are divided along slab depth so the mesh size was approximately 18.75mm.

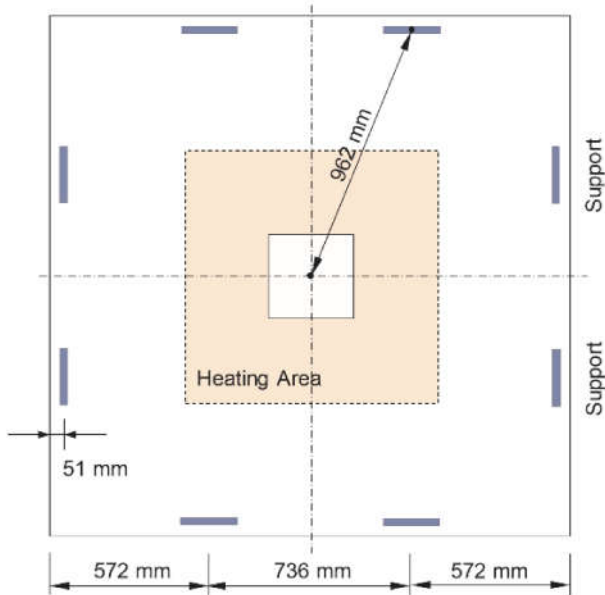


Figure 1. Plan view of experimental structure

On the other hand, in order to make the mesh size in all three directions are almost the same, use 25 mm size mesh in both two horizontal directions. There are two types of concrete slab will be simulated in this paper, Group A, concrete compressive strength is 39MPa, reinforcement distribution is NO.3 bars @ 152mm for the top mat and NO.4 bars @ 152mm for the bottom mat. Group B, concrete compression strength is 41.2MPa, with NO.3 bars @ 152mm for the top mat and NO.4 bars @ 89mm for the bottom mat, so the reinforcement ratio are 1% for Group A and 1.8% for Group B. Due to the presence of reinforcement has very few contribution to the heat transfer process of a reinforced concrete slab<sup>[6]</sup> and both the top and bottom reinforcement ratio of slab was not high, the reinforcement bars could be neglected from the heat transfer analyses. Neglecting free water evaporation in the heating process due to this effect to the result is small as well. Use 2400 kg/m<sup>3</sup> as the concrete. Both specific heat and thermal conductivity defined according to ASCE<sup>[7]</sup>. All the temperature data are acquired by the NI data acquisition system at the heated slab top face was applied as temperature boundary condition in the simulations. Introduce heat convection transfer coefficient in order to explain the heat transfer between the concrete surface and the air. All unheated specimen surfaces are assigned with a heat convection transfer coefficient of 20 J/(m<sup>2</sup>C) and 15 J/(m<sup>2</sup>C) to compare the simulation results to experimental results, because these two values are most commonly used in heat transfer analysis for concrete. From the Figure 2 (a)

and Figure 2 (b), greater heat convection transfer coefficient means lower temperature in concrete and 20 J/(m<sup>2</sup>C) is more suitable for concrete heat transfer. In general, the simulation results predict the temperature of concrete slab is a little higher than the experiment results. It is possible that the concrete thermal properties defined by ASCE does not consider the water evaporation effects. As it is shown in the figure, the simulation results have not a plateau when the temperature attains to 100°C temperature in the middle of slab and this temperature is boiling temperature of water. This maybe the main reason that the simulation results overestimated the temperature by around 53°C at 25 mm below slab heated face, 55°C in the middle of slab and 30°C at bottom face with heat convection transfer coefficient of 20 J/(m<sup>2</sup>C).

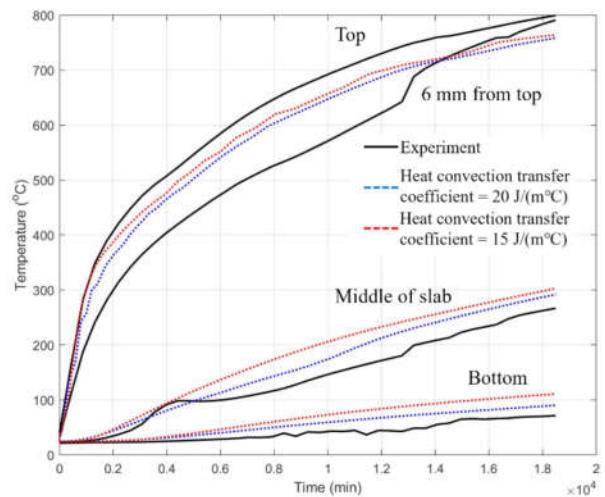


Figure 2(a). Comparison between simulated and measured temperature history of Group A

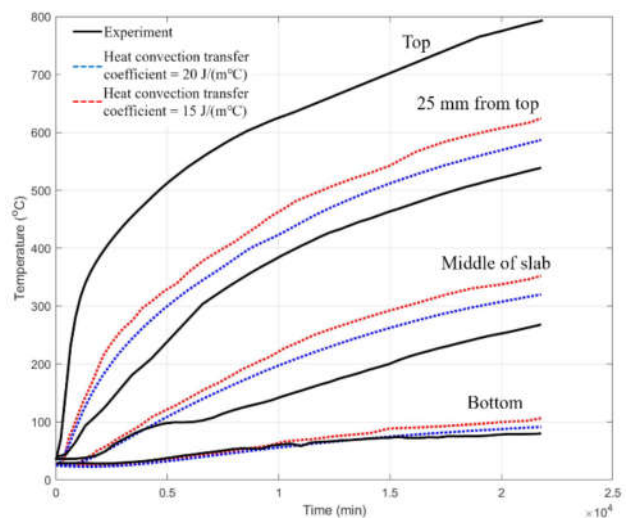


Figure 2(b). Comparison between simulated and measured temperature history of Group B

Figure 3 shows the detail of temperature distribution for the whole model under Group A heating process. As it is shown in the figure, when the heated area of slab top face attains to  $800^{\circ}\text{C}$ , at the quarter height the simulation temperature exceeds  $500^{\circ}\text{C}$ , this will cause more than 50% reduction of concrete residual strength based on ACI 216<sup>[8]</sup>. Decrease of post-punching resistance should be expected according to result of heat transfer analysis, however, both the experimental and simulation results can't get this phenomenon very well.

### 3. Simulation of Loading Tests

Due to the symmetry, only one quarter of slab with the correct boundary restraints will be simulated in this part, using an equivalent displacement instead of load driven as analysis method. Dynamic explicit algorithm is used in the whole process. The mesh size is the same as heat transfer analysis. Reinforcement in the slab was modeled using embedded truss elements, the material property of steel is bilinear stress-strain relationship and 1% strain hardening ratio. Concrete was modeled using Concrete Damaged Plasticity<sup>[9,10]</sup>. Five important parameters used to define concrete material property are determined by suggestion of Polak<sup>[11]</sup>.

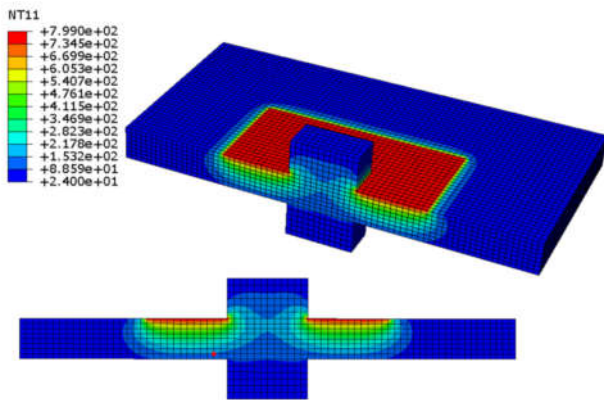


Figure 3. Predicted temperature distribution for group A specimen

(1). Dilation angle was defined as  $40^{\circ}$ , this parameter effects the result a lot; (2) Eccentricity  $e = 0.1$ . (3)  $f_{b0}/f_{c0} = 1.16$ . (4) viscosity parameter was taken as zero. (5)  $K = 0.67$ . The stress-strain relationship of concrete in room temperature is determined according to ACI 318 code<sup>[12]</sup>. Stress-strain relationship of concrete after cooling from different temperatures is determined by the experimental data given by Lee et al<sup>[13]</sup>. The temperature of each layer is based on the average value of nodal temperature between the layers. Concrete compression property was defined by stress-strain relationship as shown in Figure 4, and the

tension part was defined by tension fracture energy built-in ABAQUS. The material parameter of concrete tension part is shown in Table 1. As the temperature increase from room temperature to above  $700^{\circ}\text{C}$ , then cooling to the room temperature, the residual strength of concrete is shown through stress-strain relationship in Figure 4. Concrete material property of Group B is defined with the same method.

Temperature ( $^{\circ}\text{C}$ )	Tension (MPa)	Tension Fracture Energy (TFE)
T = 24	0.83	0.55
T = 121	0.83	0.55
T = 165	0.83	0.55
T = 217	0.79	0.52
T = 280	0.70	0.49
T = 356	0.66	0.45
T = 451	0.54	0.31
T = 570	0.32	0.2
T = 716	0.22	0.2

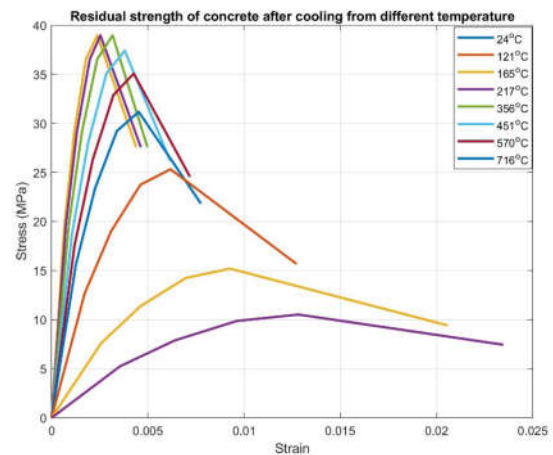
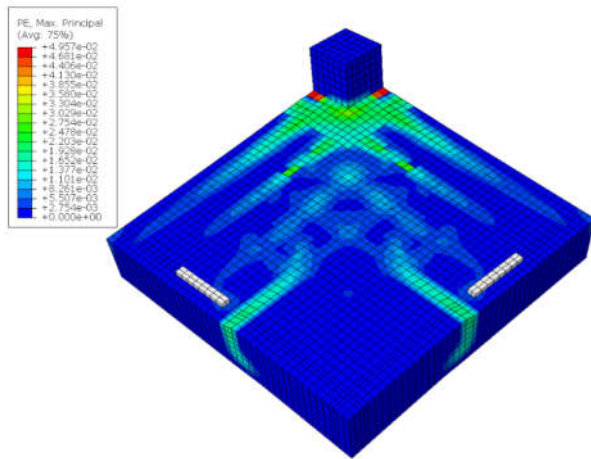
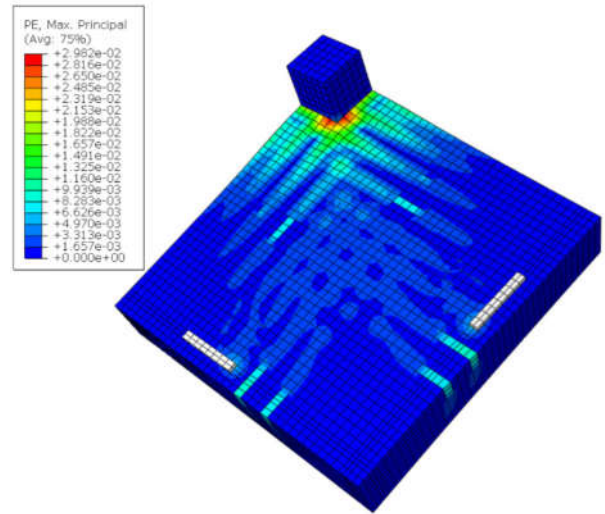


Figure 4. Stress-strain relationship for Specimen A concrete after cooling from different temperature

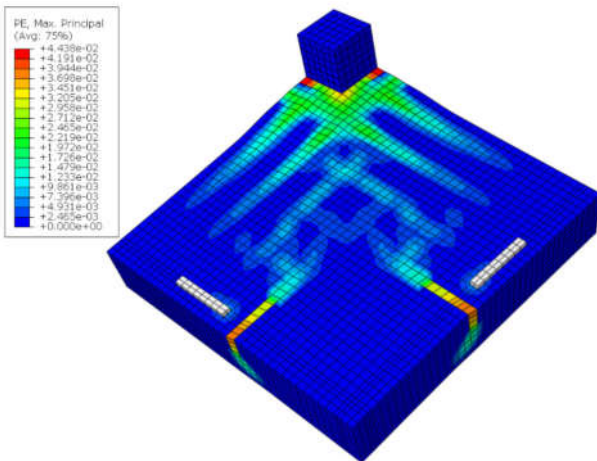
Loading simulation is performed after the all the material property have been determined, the slab is divided by 8 layers, each layers property is defined by the same as Figure 4 and Table 1, the results of both unheated and cooling after heated is shown in the Figure 5. When the maximum principle plastic strain becomes positive, concrete cracking occurs. Maximum principal plastic strain of both Group A and Group B specimen after cooling from high temperature is smaller than the unheated specimen, and loading capacity is in the same trend.



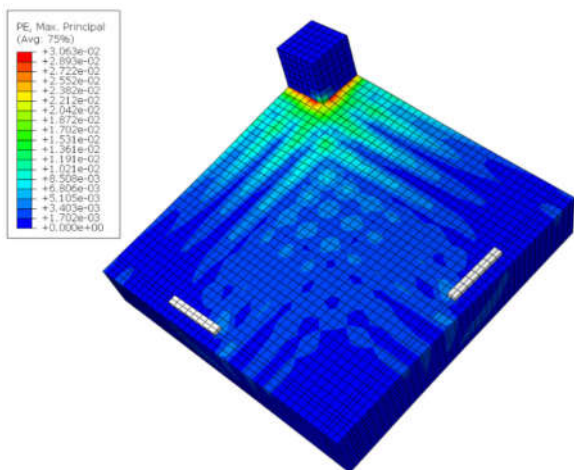
(a) Group A without experience Temperature



(d) Group B without experience Temperature



(b) Group A after cooling from high temperature



(c) Group B without experience Temperature

Figure 5. Cracking pattern in tension surface at the punching failure of Group A and B specimen

Due to the top layer of reinforcement distribution is the same in Group A and B, the stress in bottom layer of reinforcement is shown in Figure 6. The result is the same as the experiment result, in the real experiment, there are two reinforcements are broken in both Group A and B. From the simulation results, the there are two bars' stress greater than the yield strength 70ksi.

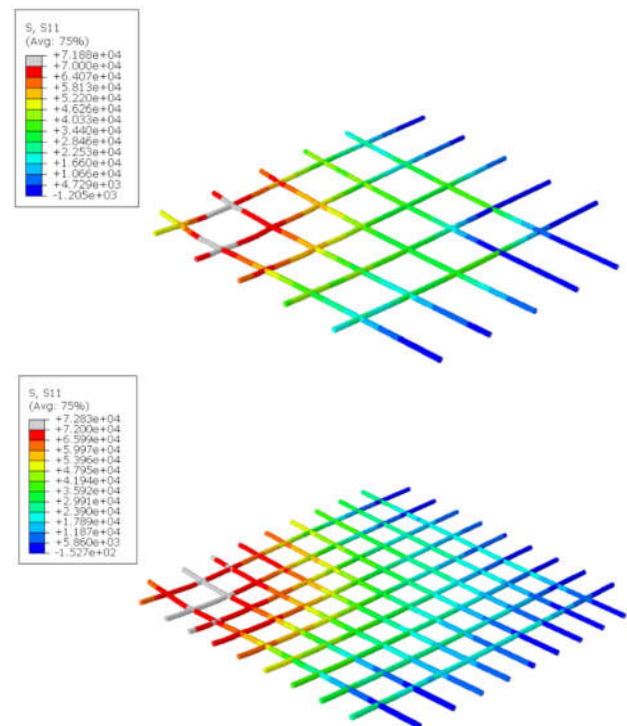
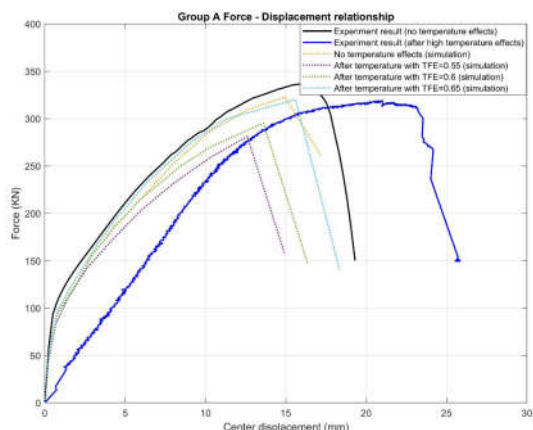
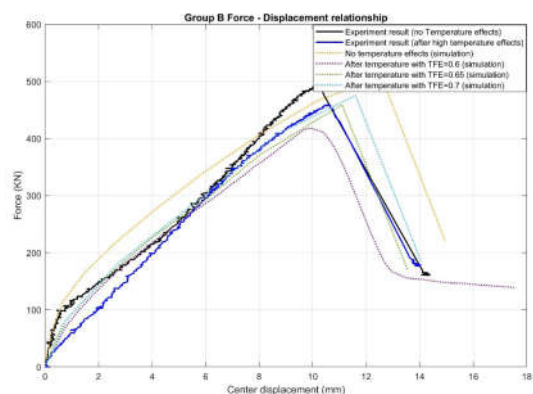


Figure 6. Stress distribution of reinforcement in the bottom layer after cooling from high temperature

Concrete loading capacity doesn't change after cooling from temperature, this phenomenon can be achieved by changing the tension fracture energy in ABAQUS. This parameter effects both the linear and nonlinear part of Force displacement curve as shown in Figure 7 and Figure 8 as shown below.



**Figure 7.** Comparison between experimental results and simulation results of Group A specimen



**Figure 8.** Comparison between experimental results and simulation results of Group B specimen

#### 4. Conclusion

(1) Finite element simulation can predict the punching capacity of slab – column connections in room temperature well. However, the simulation underestimated the residual punching strength a little. This problem can be solved by modify the dilation angle and tension fracture energy (TFE) in the software

(2) Based on the simulation result, increase the dilation angle of concrete in the simulation process can improve the loading capacity of concrete and extend the non-linear behavior of concrete as well.

(3) Modify the tension fracture energy of concrete ma-

terial can also improve the loading capacity and non-linear behavior of concrete. It makes the simulation result more like the experimental result. Find the optimized combination values of dilation angle and TFE is the best way to get the better simulation results.

#### References

- [1] Chunyu Zhang, Wenchen Ma. (2019). "Effects of high temperature on residual punching strength of slab-column connections after cooling and enhanced post-punching load resistance." *Engineering Structures* 2019; 199(15)
- [2] Ruiz, M. F., Muttoni, A., and Kunz, J. (2010). "Strengthening of flat slabs against punching shear using post-installed shear reinforcement." *ACI Structural Journal*, 107(4), 434–442.
- [3] Li, Y.-H. and Franssen, J.-M. (2011). "Test results and model for the residual compressive strength of concrete after a fire, " *Journal of Structural Fire Engineering*, 2(1), 29–44.
- [4] ABAQUS Analysis user's manual 6.10-EF, Dassault Systems Simulia Corp., Providence, RI, USA; 2010.
- [5] Wenchen Ma. (2016). "Simulate initiation and formation of cracks and potholes"
- [6] George, S. J. and Tian, Y. (2012). "Structural performance of reinforced concrete flat plate buildings subjected to fire, " *International Journal of Concrete Structures and Materials*, 6(2), 111–121.
- [7] ASCE. (1992). *Structural fire protection. Manual No. 78.* New York: ASCE Committee on Fire Protection, Structural Division, American Society of Civil Engineers.
- [8] Joint ACI-TMS Committee 216 (2007). "Code requirements for determining fire resistance of concrete and masonry construction assemblies (ACI-TMS 216.1-07)," Farmington Hills, MI, 2007.
- [9] Lubliner, J., Oliver, J., Oller, S., and Oñate, E. (1989). "A plastic-damage model for concrete." *International Journal of Solids and Structures*, 25(3), 299-329.
- [10] Lee, J., and Fenves, G.L. (1998). "Plastic-damage model for cyclic loading of concrete structures." *Journal of Engineering Mechanics*, 124(8), 892-900.
- [11] Genikomsou, A. S. and Polak, M. A. (2015). "Finite element analysis of punching shear of concrete slabs using damaged plasticity model in ABAQUS." *Engineering Structures*, 98, 38-48.
- [12] ACI (American Concrete Institute). *Building code requirements for structural concrete and commentary.* ACI 318-14, Farmington Hills, MI; 2014.
- [13] Lee J., Xi, Y., and Willam, K. (2008). "Properties of Concrete after High-Temperature Heating and Cooling." *ACI Materials Journal*, 105(4), 334-341.